Strong segregation by a migrating boundary and the decrease in electrical resistivity

1993 J. Phys.: Condens. Matter 5 4967

(http://iopscience.iop.org/0953-8984/5/28/011)

J. Phys.: Condens. Matter 5 (1993) 4967–4974. Printed in the UK

Strong segregation by a migrating boundary and the decrease in electrical resistivity

I Nakamichi

Cryogenic Centre and Faculty of Science, Hiroshima University, Higashi-Hiroshima 724, Japan

Received 10 November 1992, in final form 2 April 1993

Abstract. The residual electrical resistivity ρ has been measured with a SQUID for each small part of the specimen with a grain boundary (B part) and that of each grain on an Al–106 at.ppm Ag plate, to study boundary segregation. The annealing time is varied up to 9 d at 873 K after grain growth, and two types of cooling—rapid and slow (in a furnace)—are used. The experiment demonstrates that the migrating boundaries cause a large amount of segregation; the amount corresponds to 39–50 layers of solute. A decrease in ρ is found for the B part when it is furnace cooled, suggesting that the ρ of solute segregating about boundaries becomes an order of magnitude smaller.

1. Introduction

Both the solute segregation on a migrating boundary and the segregation effect on electrical resistivity have been studied by Kasen (1970a, b, 1972, 1983) only. Aluminium and copper with fine grains (0.1–1 mm size) have been shown to have resistivity minima during a series of anneals which have brought about grain growth. The minima have been proposed to be caused by the following two mechanisms, which are very important and fundamental (Kasen 1970b, 1972, 1983).

(1) The solute resistivity becomes zero at boundaries.
(2) The migrating boundaries cause segregation much more than equilibrium segregation.

On the assumption that mechanism (1) occurs, the magnitude of the minima corresponds to a monolayer of solute. This is orders of magnitude larger than that on equilibrium segregation.

However, the experiments seem to have several uncertainties. Firstly, the estimation of segregation is based on the assumption of mechanism (1). Secondly, the constitution of the segregation on various types of boundary in polycrystalline specimens may vary during grain growth, and this might cause the resistivity minima, because boundary resistivities depend on the boundary type and structure (Nakamichi and Kino 1986, Nakamichi 1990). Thirdly, the large amount of segregation observed might be due to the dragging of solute atoms by vacancies annihilated at boundaries during cooling (referred to as vacancy drag). Vacancy drag is known to occur during cooling when the solute–vacancy binding energy is positive, causing strong and broad segregation which extends over 0.1 mm in width in some cases (Aust *et al* 1968, Anthony 1975, Doig and Flewitt 1981).

The aim of the present experiment is to clarify whether mechanisms (1) and (2) exist, using a new method which does not have the above uncertainties. Differently from the

0953-8984/93/284967+08$07.50

previous method which measures the whole resistivity of a polycrystalline specimen during grain growth, I have measured the resistivity of each part of the specimen with a boundary and that of each grain on the specimen after grain growth, using a SQUID. Here, the small part of the specimen with a boundary is referred to as the B part. The amount of segregation is obtained without using the assumption of mechanism (1). Heat treatments have been varied in clean vacuum to determine the origin of segregation. For the specimen, Al–106 at.ppm Ag alloy was chosen for the following reasons.

(1) Vacancy drag is expected to occur in Al–Ag because the Ag–vacancy binding energy is about 0.4 eV at 850 K according to Takamura *et al* (1978).

(2) Although concentrated Al–Ag has Guinier–Preston (GP) zones and increases its resistivity on initial zone formation, Al–Ag has been shown to have a specific solute resistivity of solid solution up to the concentration of 106 at.ppm Ag at least when furnace cooled (i.e. slowly cooled) (Nakamichi 1989).

2. Experimental procedures

The Al–106 at.ppm Ag polycrystalline plates with a cross section of 1×2 mm^2 were prepared from silver of purity 99.999% and zone-refined Al with a bulk resistance ratio of 18 000 (Nakamichi and Kino 1988). Grains in the plate were grown to tens of millimetres in length by the strain-annealing method using a moving furnace in which the highest temperature was 873 K. A plate with two boundaries (GB39 and GB40) nearly perpendicular to the plate axis was selected as the specimen. GB39 is an incoherent twin boundary with the plane deviating from (111) by 3°, and GB40 is a large-angle boundary with a rotation angle of 57°. These were determined from x-ray diffraction analysis with a precision better than 1°. The specimen received a series of anneals at 873 K (except for the third anneal which was at 853 K) in a vacuum of better than 1×10^{-4} Pa using a turbomolecular pump. Then the specimen was cooled to room temperature at two different rates. The cooling rates from 873 to 673 K were 2.4 K min^{-1} (furnace or slow cooling) and 18 K min^{-1} (rapid cooling), and the details are shown in table 1. The rapid cooling was aimed at reducing vacancy drag because the segregation by vacancy drag decreases with increasing cooling rate (Doig and Flewitt 1981, Cai 1991). These heat treatments HT1–HT5 are listed in table 2 in order. It is noted that no boundary migration was observed during the above series of anneals and cooling processes.

Table 1. Data on two types of cooling. The time and cooling rate are given for each temperature range. On rapid cooling, the specimen was air quenched from 355 K.

Temperature range (K)	Furnace (slow) cooling		Rapid cooling	
	Time (min)	Cooling rate (K min^{-1})	Time (min)	Cooling rate (K min^{-1})
873–823	16.0	3.13	2.5	20.0
823–773	18.4	2.72	2.5	20.0
773–723	24.0	2.08	3.0	16.7
723–673	26.8	1.87	3.0	16.7
673–573	70	1.4	6.0	16.7
573–473	103	0.97	9.5	10.5
473–373	198	0.51	13.5	7.4
373–306	474	0.14		
373–355	...	...	6.0	3.0

Table 2. Details of heat treatments. The specimen received heat treatments in the order of the HT number.

Heat treatment	Annealing temperature (K)	Each annealing time (min)	Total annealing time (min)	Cooling method
HT1	873	30	30	Rapid cooling
HT2	873	35	65	Furnace cooling
HT3	853	540	605	Furnace cooling
HT4	873	5760	6365	Furnace cooling
HT5	873	6900	13265	Rapid cooling

The resistance $R(4.2\ \mathrm{K})$ at 4.2 K was measured using an SHE model PMS-330 SQUID system with a sensitivity of 3×10^{-13} V for the five parts of the specimen shown in figure 1, after each anneal. To obtain the size factors of these parts, their resistances $R(300\ \mathrm{K})$ at 300 K were measured with an Otto–Wolff KDE 84 potentiometer having a sensitivity of 3 nV. The measurement was made in an oil bath regulated at 300 ± 0.01 K after the first anneal. A further drift in the bath temperature was detected with an Al wire and was corrected by measuring simultaneously the resistances of the wire and the specimen.

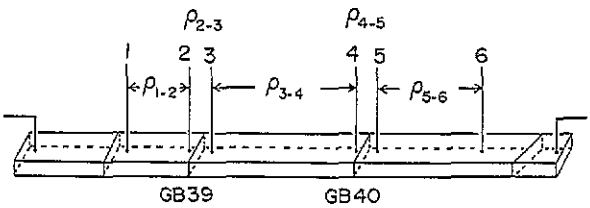

Figure 1. Specimen used for electrical resistivity measurement. ρ_{1-2}, ρ_{2-3}, etc, are the residual resistivities between PL1 and PL2, between PL2 and PL3, etc, respectively; the leads are made of the same material as the specimen and spot welded.

With these resistances, the residual resistivity ρ was estimated from

$$\rho = 27.26\ \mathrm{n\Omega\ m} \times R(4.2\ \mathrm{K})/R(300\ \mathrm{K}) \tag{1}$$

where 27.26 nΩ m is the resistivity of Al–106 at.ppm Ag determined previously using a wire (200 mm in length and 1 mm in diameter) of the same material as used in the present work (Nakamichi and Kino 1988). The relative error of the residual resistivity obtained was ±0.01%.

The specific boundary resistivity ρ_{gb} is defined as the resistivity per unit area of the boundary perpendicular to the current flow in unit volume. ρ_{gb} for GB39 is deduced from the ρ_{2-3} of the B part between potential lead 2 (PL2) and potential lead 3 (PL3), and from the ρ_{1-2} and ρ_{3-4} of contiguous grains, using the following equation (see figure 1):

$$\rho_{2-3} - (\rho_{1-2} + \rho_{3-4})/2 = \rho_{gb} S/V \tag{2}$$

where S is the cross-sectional area of the specimen and V is the volume between PL2 and PL3. The factor S/V is equal to $1/L_{2-3}$, where L_{2-3} is the length between PL2 and PL3. The length L_{2-3} was determined to be 1.71 mm from the resistances R_{1-6} and R_{2-3} at 300 K and the length L_{1-6} was measured with a travelling microscope. Similarly, ρ_{gb} for GB40 was deduced from the ρ of the B part between PL4 and PL5 and from those of contiguous grains, where $L_{4-5} = 1.49$ mm. More experimental details have been described elsewhere (Nakamichi and Kino 1986, Nakamichi 1990).

3. Results and discussion

3.1. Estimation of the segregated-solute distribution varied by heat treatments

First, we estimate the variation in the segregated-solute distribution due to the heat treatments. This is necessary to interpret the boundary resistivity correctly. The anneal at 873 K makes the segregated solute diffuse from the boundaries towards grains. This profile can be approximately estimated with the following equation due to Shewmon (1963). He has treated the diffusion of solute inserted as a thin film in the middle of a long bar of solute-free material initially. The equation gives the solute concentration c along the bar annealed for time t:

$$c = (A/2\sqrt{\pi Dt})\exp(-x^2/4Dt) \tag{3}$$

where A is the quantity of solute of film inserted initially, D is the diffusion coefficient at the annealing temperature and x is the distance in either direction normal to the solute film. This equation also gives the maximum concentration as $A/2\sqrt{\pi Dt}$, and the width w of the solute distribution can be taken as

$$w = 4\sqrt{Dt} \tag{4}$$

because c at $x = 2\sqrt{Dt}$ is $1/e$ of that at $x = 0$.

Figure 2 is the schematic plot of the variation in segregated-solute distribution, which is estimated with equation (3) using each annealing time for HT1–HT3 in table 2. The silver is assumed to segregate at boundaries as a silver film initially. The value of A is taken to be 14 nm, equal to a silver film of 14 nm thickness. This is from the value of ρ_{gb} obtained for GB39, which will be shown later. For the value of D ($m^2\ s^{-1}$), the following experimental equation for Ag in Al is used (Peterson and Rothman 1970):

$$D = 1.18 \times 10^{-5}\exp(-E/kT) \tag{5}$$

where the activation energy $E = 1.933 \times 10^{-19}$ J K^{-1} (= 1.206 eV) and k is the Boltzmann constant. The figure is for GB39 but the situation is nearly the same for GB40 also. The inset shows w defined by equation (4).

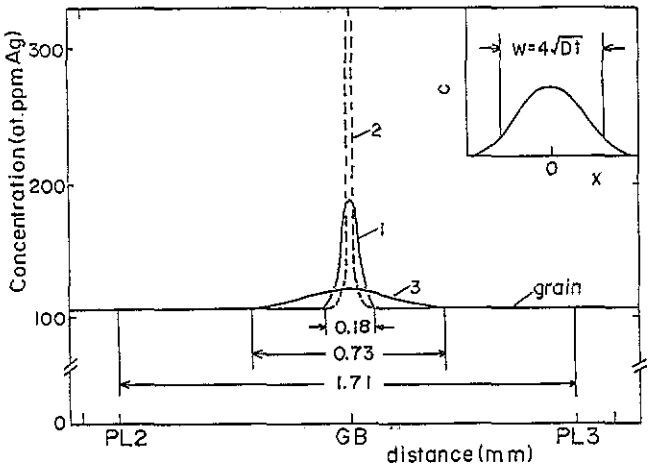

Figure 2. Schematic plot of the segregated-solute distribution varied by diffusion due to heat treatments. This is estimated for GB39 using equation (3) for the three heat treatments in table 2, where the appropriate annealing time is used. The broken curve is due to vacancy drag. The HT numbers are shown beside the curves. The inset shows the segregated-solute distribution width w.

As to the segregation due to vacancy drag, the uncertainties in the Ag–vacancy binding energy give an unreliable estimation. However, the calculation of the diffusion distance of silver to boundaries can give reliable information, because the main factors in vacancy drag such as Ag–vacancy binding and migration are reflected in the diffusion coefficient D. In addition, the cooling rates in the present experiment are relatively small. Thus, the vacancies are considered to possess nearly thermal equilibrium concentrations, the same as in the experiment determining equation (5). For the boundary sink, the diffusion equation for a semi-infinite solid is applicable. This shows that solute–vacancy complexes at a distance of $2\sqrt{Dt}$ from the boundary can reach it (Shewmon 1963, Doig and Flewitt 1981, Cai 1991).

Using equation (5) and table 1, the sum L_v of $2\sqrt{Dt}$ during cooling is calculated where, for T in equation (5) and t, the average of the highest and lowest temperatures in each temperature range and the time of range, respectively, are taken. The L_v obtained are 0.132 mm and 0.048 mm for furnace (slow) cooling and rapid cooling, respectively. This suggests that the vacancy-drag segregation is about three times larger on furnace cooling than on rapid cooling. Unless vacancy drag occurs, the curve for HT2 will have a maximum of 160 at.ppm and a width w of 0.27 mm according to equation (3). This w is twice the $L_v = 0.132$ mm for furnace cooling. Since Ag–vacancy complexes move towards a boundary from both sides of the grains, this means that vacancy drag can return most of the silver which has been diffused out to boundaries on HT2, if it is operative. The above suggests that the vacancy-drag segregation is most effective on HT2 of the three heat treatments for furnace cooling. Thus, this is schematically plotted as a broken curve for HT2 in figure 2.

Figure 2 shows the following.

(1) On HT1, the anneal diffuses the segregated silver to a width of 0.18 mm, bringing about a large decrease in the concentration. The rapid cooling would not change this situation much, compared with the subsequent furnace cooling.

(2) On HT2, the furnace cooling is expected to cause large vacancy-drag segregation as shown by the broken curve.

(3) On HT3, the long-time anneal diffuses the segregated silver up to a width of 0.72 mm, decreasing the concentration near to that of the grains as shown by curve 3. In this case, the vacancy-drag segregation must be much smaller than on HT2, because the segregated silver diffuses widely and its concentration is much decreased. Thus, curve 3 can be regarded as nearly the same as the curve after cooling.

Figure 2 also shows two important features about HT1–HT3.

(1) The segregated solute does not diffuse out of the B part between PL2 and PL3.

(2) The segregated solute is in the solid-solution state except on HT2.

Because curves 1 and 3 have smaller concentrations than the lattice solubility of Al–Ag alloy at 300 K; the solubility is estimated to be about 200 at.ppm Ag by the extrapolation of the data in the book by Hansen and Anderko (1958). In addition, since the real initial segregation is probably not so dense as the solute film used for the initial condition in the estimation, the real concentrations corresponding to curves 1 and 3 must be smaller than those in the figure. Moreover, the solubility at boundaries at 300 K has been shown to be larger than the lattice solubility (Mclean 1957).

Since ρ_{gb} arises mainly from the ρ of the B part, the above features (1) and (2) allow us to estimate the amount of initial segregation using the value of ρ_{gb} and the specific resistivity of the solid solution of Al–Ag, except on HT2.

3.2. *The variation of ρ_{gb} due to heat treatment*

3.2.1. The amount of segregation and its origin. Figure 3 shows the variation in ρ_{gb} due to the heat treatments in table 2. For reference, the segregated-solute distribution width $w = 4\sqrt{Dt}$ is calculated with the total annealing time and shown at the top of the figure. The magnitude of the error bar is due to the difference between the ρ-values of two grains (cf. equation (2)); the values of ρ are shown later in figure 4 for three heat treatments.

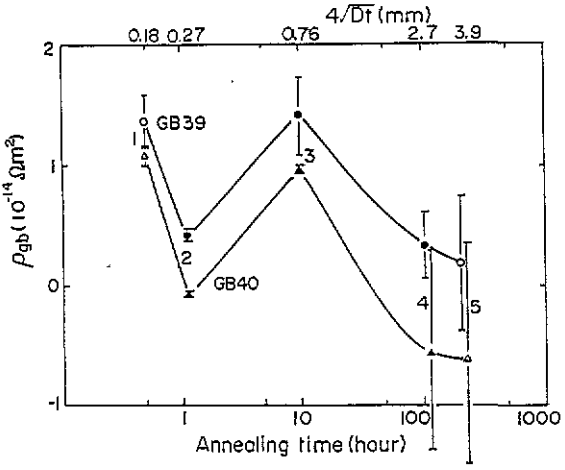

Figure 3. Variation in the specific boundary resistivity ρ_{gb} at 4.2 K plotted against the total annealing time for the heat treatments in table 2 (for Al–106 at.ppm Ag after grain growth): ○, ●, incoherent twin boundary (GB39); △, ▲, large-angle boundary (GB40): ○, △, rapid cooling; ●, ▲, furnace (slow) cooling. The HT numbers are shown beside the data points. The segregated-solute distribution width $4\sqrt{Dt}$ is calculated with the total annealing time, for reference. The magnitude of the error bar is due to the difference between the residual resistivities of two grains (cf. equation (2)).

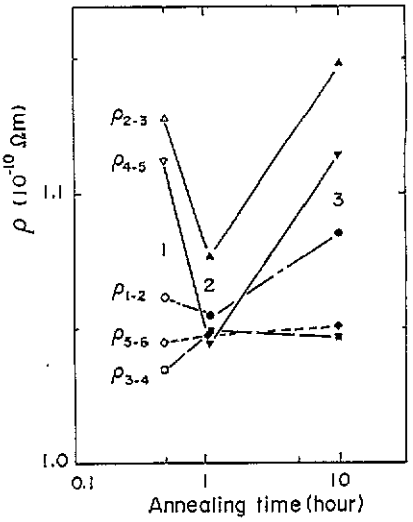

Figure 4. Variation in the residual resistivity ρ due to heat treatments in table 2 for the five parts of the specimen shown in figure 1: △, ▽, ○, ◇, □, rapid cooling; ▲, ▼, ●, ◆, ■, furnace (slow) cooling. The HT numbers are shown beside the data points.

As described in section 3.1, the amount of initial segregation can be deduced from the value of ρ_{gb} on HT1 and HT3. The fact that nearly the same values of ρ_{gb} occur on HT1 and HT3 is consistent with the argument in section 3.1, thereby supporting it. The values of ρ_{gb} on HT1 and HT3 are tens to hundreds of times larger than those for pure Al which are equal to 10^{-16}–10^{-17} Ω m^2 (Kasen 1970a, b, Nakamichi 1990). Thus, ρ_{gb} arises mainly not from the boundary but from the segregated solute. That is, ρ_{gb} is due mainly to the difference between the solute resistivity of the B part and that of the contiguous grains in this alloy (see equation (2)). Thus, we can take ρ_{gb} as equal to the amount of segregated solute multiplied by the specific solute resistivity. Using the specific resistivity of Ag in Al which is equal to 10.0 nΩ m (at.%)$^{-1}$ (Nakamichi 1989), the ρ_{gb}-value of 1.4×10^{-14} Ω m^2 for GB39 corresponds to a length of 14 nm (50 layers) of Ag. For GB40, ρ_{gb} is 1.1×10^{-14} Ω m^2, corresponding to 39 layers of Ag. Similar a large ρ_{gb} (corresponding to ten layers of Ag) has been observed even for the Al–50 at.ppm Ag bicrystals, for which the heat treatment was nearly the same as HT3, confirming the present work (Nakamichi 1990).

On HT4 and HT5, ρ_{gb} becomes much smaller than those on HT1 and HT3. As seen from the data on HT4, the vacancy drag on furnace cooling does not change this feature. On

HT4 and HT5, since w becomes larger than the length of the B part ($L_{2-3} = 1.71$ mm and $L_{4-5} = 1.49$ mm), this feature must be due to the diffusion of the initially segregated solute, from the B part to the grains. Thus, this demonstrates that the large amount of segregation observed is not due to the vacancy drag during cooling but mainly to the segregation by the migrating boundary.

As described above, the present result is consistent with mechanism (2). However, the segregation corresponds to 39–50 layers of solute. This is beyond Kasen's (1972, 1983) more detailed proposal that moving boundaries interact thermodynamically with the impinging solute field in a manner similar to that of a stationary boundary in a steadily increasing solute field; the maximum segregation by this mechanism is a monolayer of solute which is the full boundary saturation predicted by Mclean (1957). On the other hand, it has been shown that migrating boundaries absorb and generate vacancies (Gottschalk *et al* 1980, Lücke and Gottstein 1981) and that incoherent twin boundaries are also good sinks for vacancies (Siegel *et al* 1980). Thus, it is suggested that migrating boundaries interact with solute atoms through the vacancies associated with boundary migration and cause large segregation when the solute–vacancy binding energy is positive.

3.2.2. Resistivity decrease on segregation. As seen in figure 3, ρ_{gb} is drastically decreased by the furnace cooling on HT2. The ρ_{gb} for GB40 and GB39 become about 0 and $\frac{1}{3}$, respectively. The resistivities recover to the initial level again on HT3.

In order to check whether the above large decrease in ρ_{gb} arises from an extrinsic reason such as contamination or surface oxidation, the variations in ρ of five parts of the specimen are shown for HT1–HT3 in figure 4 (cf. figure 1). Both the resistivities ρ_{2-3} and ρ_{4-5} of B parts are decreased by 5–6% on HT2 and recover again on HT3. In comparison with this, the resistivities ρ_{1-2}, ρ_{3-4} and ρ_{5-6} of grains hardly vary during HT1–HT3. These show that the ρ_{gb} decrease on HT2 is intrinsic.

On HT2, the vacancy drag during furnace cooling is expected to return much of the silver, which was segregated by migrating boundaries originally and diffused nearby, to boundaries, as described in section 3.1 (see figure 2). Even if the vacancy drag is not effective, the silver segregated by migrating boundaries may remain near to them because the annealing time is short. Therefore, the specific resistivity of the solute segregating about boundaries is suggested to become an order of magnitude smaller than that of the solid solution, when furnace cooled.

This resistivity decrease cannot be explained by the change in boundary strain field due to segregation, because the long-range strain field of boundaries or dislocations hardly contributes to resistivities (Brown 1982, Watts 1989, Nakamichi 1990). Moreover, even if the solute completely loses the resistivity contribution when captured by boundary strains as assumed by Kasen (1970b), it explains only 10% of the observed resistivity decrease because the volume summation of the boundary strains corresponds to a few layers of solute at most (Webb 1957). In addition, the increase in ρ_{gb} on HT3 also does not seem to be due to the formation of a GP zone, because the solute concentration of the B part is near to that of grains on HT3 as shown in figure 2, and the specific solute resistivity of Al–106 at.ppm Ag has been verified to be the same as that of the solid solution, as noted in the introduction.

The resistivity decrease might be due to precipitation (or clustering) about boundaries during furnace cooling. The cooling has a very slow rate below 373 K, as seen in table 1. Recently, Osono *et al* (1992) have observed a decrease in resistivity at a temperature of 378–300 K during the very slow cooling (step cooling) of an Al–0.1 at.% Ag polycrystal and attributed this to the formation of precipitates; on step cooling, the specimen temperature

was kept constant for 24 h every 5 K during cooling in the furnace. The silver in precipitates has been shown to have a specific resistivity of a tenth of that of the solid solution. The precipitates or clusters may be helped to form by vacancy drag, because it helps the solute atoms to meet and to interact through transportation of solute to boundaries.

Theoretically, when solute atoms segregate, the distance between them becomes very short and the scattering waves from each solute atom can interact with each other. Hillel and Rossiter (1981) and Rossiter (1987) have shown that the interference of scattering waves decreases or increases the resistivity, depending on the structure factor of the solute system. According to their theory, this interference occurs when the distance between solute atoms is smaller than the electron mean free path. Since the mean free path at 4.2 K in this alloy is of the order of micrometres (Nakamichi 1989) and the distance between the nearest solute atoms is of the order of nanometres on average even for a concentration of 0.1 at.%, interference can occur.

Therefore, the resistivity decrease observed probably arises from the interference of scattering waves between the segregated solute atoms. This phenomenon may even reduce the ρ of the B part to smaller than that of grains, leading to a negative ρ_{gb}. The effect of scattering wave interference may depend on the segregated-solute morphology, which includes the case of clusters and precipitates, as predicted by Rossiter (1980) for ordering and clustering. More detailed experiments will be carried out on this point.

References

Anthony T R 1975 *Diffusion in Solids* (New York: Academic) p 353
Aust K T, Hanneman R E, Niessen P and Westbrook J H 1968 *Acta Metall.* **16** 291–302
Brown 1982 *Can. J. Phys.* **60** 766–78
Cai W 1991 *J. Phys.: Condens. Matter* **3** 609–12
Doig P and Flewitt P E J 1981 *Acta Metall.* **29** 1831–42
Gottschalk C, Smidoda K and Gleiter H 1980 *Acta Metall.* **28** 1653–6
Hansen M and Anderko K 1958 *Constitution of Binary Alloys* 2nd edn (New York: McGraw-Hill)
Hillel A J and Rossiter P L 1981 *Phil. Mag.* B **44** 383–8
Kasen M B 1970a *Phil. Mag.* **21** 599–610
—— 1970b *Scr. Metall.* **4** 575–80
—— 1972 *Acta Metall.* **20** 105–13
—— 1983 *Acta Metall.* **31** 489–97
Lücke K and Gottstein G 1981 *Acta Metall.* **29** 779–89
Mclean D 1957 *Grain Boundaries in Metals* (Oxford: Oxford University Press)
Nakamichi I 1989 *J. Phys.: Condens. Matter* **1** 8887–99
—— 1990 *J. Sci. Hiroshima Univ.* A **54** 49–84
Nakimichi I and Kino T 1986 *Trans. Japan. Inst. Met. Suppl.* **27** 1013–20
—— 1988 *J. Phys. F: Met. Phys.* **18** 2421–8
Osono H, Hashimoto E, Kawata S and Kino T 1992 *Phys. Status Solidi* **129** 399–408
Peterson N L and Rothman S J 1970 *Phys. Rev.* **1** 3264–73
Rossiter P L 1980 *Phil. Mag.* B **42** 561–4
—— 1987 *The Electrical Resistivity of Metals and Alloys* (Cambridge: Cambridge University Press)
Shewmon P G 1963 *Diffusion in Solids* (New York: McGraw-Hill)
Siegel R W, Chang S M and Balluffi R W 1980 *Acta Metall.* **28** 249–57
Takamura J, Koike M and Furukawa K 1978 *J. Nucl. Mater.* **69–70** 738–40
Watts B R 1989 *Conduction Electron Scattering in Dislocated Metals* (Amsterdam: Elsevier)
Webb W W 1957 *Acta Metall.* **5** 89–96